EXPERIMENTAL AND NUMERICAL STUDY OF TURBULENT NEWTONIAN FLOW THROUGH AN AXISYMMETRIC SUDDEN CONTRACTION

Fredy Palacios Sánchez, fremps@hotmail.com
João Luiz Noguchi Machuca, jmachuca@utfpr.edu.br
Admilson T. Franco, admilson@utfpr.edu.br
Rigoberto E. M. Morales, rmorales@utfpr.edu.br
Universidade Tecnológica Federal do Paraná-UTFPR, Curitiba-Pr 80230-901, Brasil

Abstract. *Turbulent flows through sudden contractions are common in many industrial applications including piping systems, aeronautics, slurry transportation, molding and extrusion. The contraction causes pressure losses and influences the flow pattern at the upstream and downstream regions from the contraction plane. In this work, numerical and experimental tests were performed in a sudden contraction of contraction ratio* $\beta=1.97$. *Two turbulence models were used, namely, the algebraic LVEL model and the two-equation k-ε turbulence model. The balance equations were discretized using the finite volume method and the hybrid interpolation scheme. The Particle Image Velocimetry technique (PIV) was used to obtain the two-dimensional velocity field along the upstream region. Pressure loss coefficients were obtained experimentally for upstream Reynolds numbers* Re_D *in the range of 15,000 to 40,000. Experimental and numerical velocity vetors in different positions along the upstream region were obtained for* Re_D *=17,800, 24,600 and 40,000. Comparison between numerical and experimental velocity profiles yielded good agreement, despite some differences close to the plane contraction. Pressure loss coefficients measured experimentally showed good agreement when compared with previous works. Comparison between the numerical results of k-ε-LB and L-VEL turbulence models with experimental data for the velocity profiles and contraction loss coefficients showed a better adjustment with the k-ε-LB model. Based on the PIV measurements and in contrast with previous works, the presence of a vortex imediately prior to contraction was observed for all* Re_D *investigated.*

Keywords*: axisymmetric sudden contraction, pressure loss coefficient, Newtonian fluids, PIV.*

1. INTRODUCTION

Fluid flows through a sudden contraction are common in many engineering applications such as piping systems, polymer processes, extrusion and molding. This kind of flow is associated with abrupt pressure drop and recirculation in the upstream and downstream regions of the contraction plane. Considering the technological importance of this geometry, many studies were developed in order to predict the fluid flow and understand the behavior and to its peculiars characteristics.

Initial studies focused on the measurement of the excess pressure drop. Astarita and Greco (1968) studied experimentally the pressure drop problem of laminar Newtonian flow through an abrupt contraction. The experiments were performed with water and glycerol solutions as working fluids, and a contraction ratio $\beta = D/d = 2.49$. The results showed two different behavior depending on the downstream Reynolds number, Re_d: for $\mathrm{Re}_d < 146$ was observed a linear decreasing of the pressure drop, while for $\mathrm{Re}_d > 146$ an approximately constant pressure drop was observed.

The development of experimental non-intrusive techniques has allowed to obtain information about the kinematic of fluid flow, like velocities profiles, turbulence intensities, and other important variables. Ramamurthy and Boger (1971) measured the velocities profiles along the downstream flow region of a contraction with $\beta = 2$ using a non-intrusive technique involving streak photography. The experiments were conducted for laminar Newtonian and inelastic polymer solutions. Results clearly showed the presence of a stationary vortex on the upstream side of the contraction for low Reynolds numbers. Furthermore, it was noticed that the vortex is absent for higher Reynolds numbers.

Durst and Loy (1985) conducted a numerical and experimental study of laminar flow in a pipe with a sudden contraction of $\beta = 1.87$. The numerical approach was performed using the finite difference scheme and the experimental investigations were carried out through LDA measurements. Tests allowed to obtain velocities profiles along the upstream and downstream regions of the contraction plane. The numerical tests provided information about the vortex region, including the length of flow separation in the concave and convex corners of the plane of contraction. Comparison between numerical and experimental results yielded good agreements for most of flow field.

In addition to the detailed study of the kinematics of the flow in a sudden contraction, recent studies have focused on determining the pressure loss coefficient, k_c. Bullen *et al.* (1987) studied numerically and experimentally the turbulent water flow in contractions with different contraction ratios, namely, $1.2 \le \beta \le 2.72$ and with the upstream

Reynolds number ranging from $4\times10^4 \le \mathrm{Re}_D \le 2\times10^5$. The results for k_c showed reasonably agreement when compared with other experiments. Also, it was observed that k_c shows dependence of Re_D, increasing its value with the reduction of Re_D. On the other hand, this dependence decreases for higher Re_D. Bullen *et al.* (1996), in a more recent study, developed a complementary work for the same Reynolds number studied in Bullen *et al.* (1987). The experimental measurements were carried out using the LDA technique for $\mathrm{Re}_D = 153{,}800$. The measurements showed the formation of the vena contracta in the downstream region, its axial position and size and the re-attachment of the uniform flow.

The present work investigates numerically and experimentally the Newtonian flow through an abrupt contraction with $\beta = 1.97$. The numerical tests are performed with Computational Fluid Dynamics (CFD) and the experimental measurements are carried out with the PIV technique. The main objective is to determine the velocity profiles in the longitudinal and radial directions along the upstream flow region of the contraction. Flow pattern along the upstream region is studied with the PIV technique in order to observe the formation of the vortex region. Also, pressure loss coefficients are obtained for different upstream Reynolds numbers, Re_D, in the range $1.7\times10^4 \le \mathrm{Re}_D \le 4\times10^4$. The numerical and experimental results are compared with previous works.

Fluid flow through an axisymmetric sudden contraction is shown in Figure 1a. The cylindrical coordinates system (r,z) is conveniently located in the plane of the contraction. The flow initially shows a fully developed behavior in the upstream region with a bulk velocity V_1, and then due to the influence of contraction, a secondary-flow vortex arises in the corner of the upstream tube of inner diameter D. Around the plane contraction, the pressure profile is dramatically affected, and then when the entry length $z = L_e$ is reached, fully developed flow condition establishes again, as shown in Figure 1b. A bulk velocity V_2 is observed in the downstream pipe of inner diameter d.

Important parameters related to the study of fluid flow through a contraction are: the contraction ratio, $\beta = D/d$, and the upstream Reynolds number, $\mathrm{Re}_D = \rho V_1 D/\mu$, where ρ and μ are the density and dynamic viscosity of the fluid, respectively.

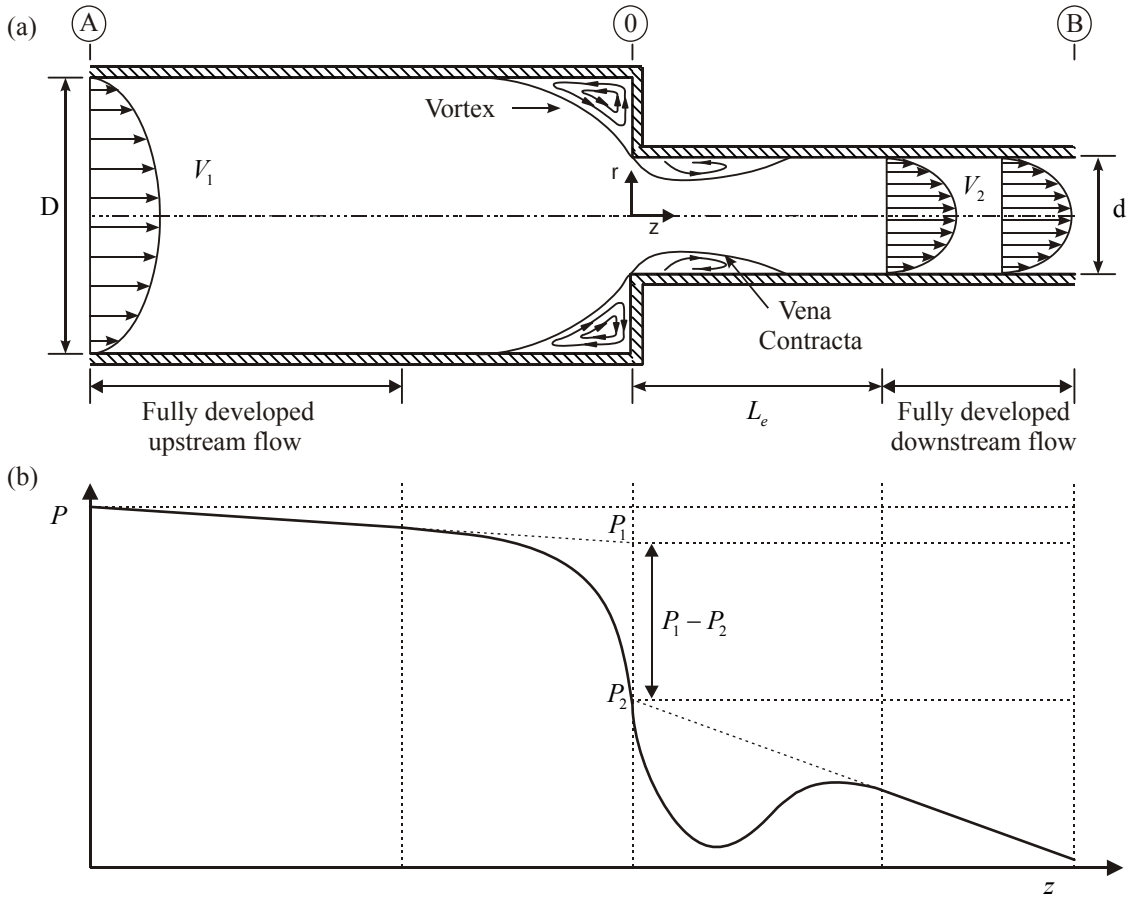

Figure 1. Schematic representation of problem definition for a sudden contraction: (a) Flow pattern and (b) Pressure profile.

2. MATHEMATICAL MODELING

The fluid is Newtonian and the flow is assumed two-dimensional and axisymmetric, incompressible, isothermal and steady state. The mass and momentum balance equations in cylindrical coordinate system can be written in the indicial form as (Wilcox, 1998):

$$\frac{\partial \overline{u}_i}{\partial x_i} + \frac{1}{r}\frac{\partial}{\partial x_j}\left(r\overline{u}_j\right) = 0 \tag{1}$$

$$\overline{u}_i \frac{\partial \overline{u}_i}{\partial x_i} + \overline{u}_j \frac{\partial \overline{u}_i}{\partial x_j} = -\frac{1}{\rho}\frac{\partial \overline{p}}{\partial x_i} + \frac{1}{r}\frac{\partial}{\partial x_j}\left[r\left(\mu + \mu_T\right)\frac{\partial \overline{u}_i}{\partial x_j}\right] \tag{2}$$

Equations (1) and (2) are not enough to solve the problem due to the turbulent regime. In that sense, equations to model the turbulent viscosity μ_T are necessary. In the present work, two turbulence models are used: the algebraic LVEL model and the two-equation, low-Reynolds-number *k-ε* turbulence model (Lam-Bremhorst, 1981). The LVEL model uses an algebraic equation called Spalding law for the calculation of μ_T, expressed by:

$$\mu_T = \mu\left(\frac{k_1}{e^{k_1 B}}\right)\left[e^{k_1 u^+} - 1 - k_1 u^+ - \frac{\left(k_1 u^+\right)^2}{2} - \frac{\left(k_1 u^+\right)^3}{6}\right] \tag{3}$$

where μ is dynamic viscosity, $k_1 \approx 0.41$ and $B \approx 5.0$ (Wilcox, 1998) are universal dimensionless constants of turbulent flows. u^+ is the dimensionless velocity, $u^+ = u / v^*$, where v^* is the friction velocity.

On the other hand, the $k-\varepsilon-LB$ two-equation model adds two differential equations to calculate the turbulent viscosity. The parameter k, which refers to the turbulent kinetic energy and ε, which represents the turbulent dissipation rate.

$$\mu_t = C_\mu f_\mu \frac{k^2}{\varepsilon} \tag{4}$$

$$\frac{\partial k}{\partial t} + U_j \frac{\partial k}{\partial x_j} = \tau_{ij}\frac{\partial U_i}{\partial x_j} - \varepsilon + \frac{\partial}{\partial x_j}\left[\left(\mu + \frac{\mu_T}{\sigma_k}\right)\frac{\partial k}{\partial x_j}\right] \tag{5}$$

$$\frac{\partial \varepsilon}{\partial t} = \frac{\partial}{\partial x_j}\left[\left(\frac{\mu_t}{\sigma_e} + \mu_t\right)\frac{\partial \varepsilon}{\partial x_j}\right] + C_{\varepsilon 1} f_1 \mu_t \frac{\varepsilon}{k}\left(\frac{\partial U_i}{\partial x_j} + \frac{\partial U_j}{\partial x_i}\right)\frac{\partial U_i}{\partial x_j} - C_{\varepsilon 2} f_2 \frac{\varepsilon^2}{k} \tag{6}$$

$C_\mu = 0.09$, $\sigma_k = 1.0$, $C_{\varepsilon 1} = 1.44$ and $C_{\varepsilon 2} = 1.92$ are closure coefficients (Launder e Spalding, 1974). The calculation procedure and further information about the functions f_μ, f_1 and f_2 are discussed by Lam e Bremhorst (1981).

For the problem illustrated in Figure 1(a), the following conditions can be applied: a no-slip condition on the walls: $r = D/2$ or $d/2$, $w = v = 0$; an entry uniform velocity profile: $z = 0$, $w = V_e$, $v = 0$ and an atmospheric pressure in the downstream outlet section: $z = L$, $P_L = P_0$. Also, the length of the upstream and downstream pipes should be long enough in order to guarantee a fully developed flow.

The pressure loss coefficient, k_c, is calculated as:

$$k_c = \frac{\left[\left(P_1 - P_2\right)/\rho g\right] + \left[\left(\overline{V}_1^2 - \overline{V}_2^2\right)/2g\right]}{\overline{V}_2^2/2g} \tag{7}$$

where ρ is the fluid density, g is the gravity, $\overline{V}_1$ and $\overline{V}_2$ are the upstream and downstream bulk velocities, respectively. The pressure values P_1 and P_2 are obtained through the pressure gradient extrapolation of fully developed flow in the downstream and upstream region of the contraction plane, as depicted in Figure 1b.

The governing equations are discretized using the finite volume method, and the hybrid scheme is used to interpolate the convective terms. The SIMPLEST algorithm (Patankar and Spalding, 1972) is used for the pressure-velocity coupling. Convergence was determined using the residual control criterion, setting a maximum of 10^{-6} for the sum of all absolute residuals of each variable (u, v, p, k, ε), below which the solution was considered converged.

3. EXPERIMENTAL SETUP

In order to carry out the experimental investigations, an especial loop was built. Figure 2 shows a schematic view of the experimental facility. The system is a closed loop composed of a series of PVC pipes, a bypass, a return line, a test section, temperature and pressure sensors, a variable-speed AC motor-driven and other devices. The upstream Plexiglas pipe has an inner diameter of $D = 23.9$ mm and a length of 5.28 m, and the downstream section is a Plexiglas pipe with a $d = 12.15$ mm inner diameter and a 3.24 m length, whose connection results in the contraction inside the visualization box of $\beta = 1.97$. The flanges and pipe junctions were carefully manufactured to ensure that no distortion occurs in the flow. The upstream and downstream pipe lengths should ensure fully developed and redeveloped flow at the inlet and at outlet sections of the contraction plane, respectively, for all cases studied. In order to obtain good pressure measurements on the pressure tapping closer to the contraction and for its posterior use in a future work with laminar regimes, the pressure tapping location was chosen considering the most conservative value given in the literature (Vrentas and Duda, 1987; Fester *et al*, 2008; Bullen *et al.*,1987 and White, 2002).

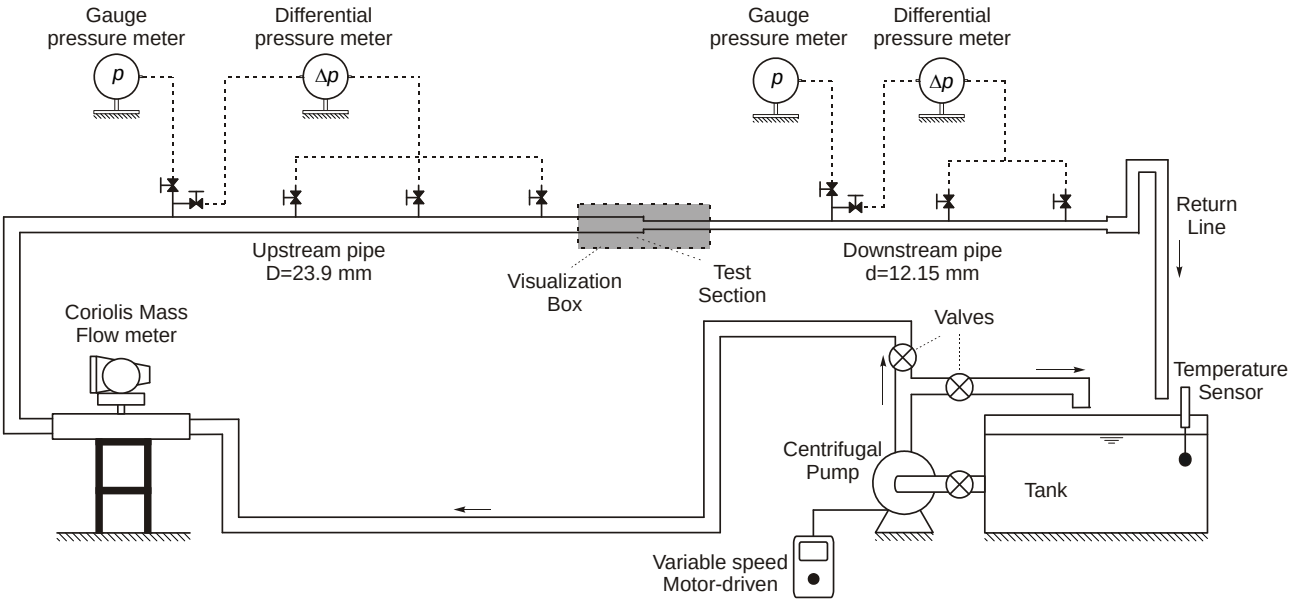

Figure 2. Schematic view of the experimental setup.

In order to minimize distortion effects of the PIV images produced by the pipe curvature and differences between refractive indexes of the fluid (n=1.33) and the Plexiglas pipe (n=1.49), it was proposed a visualization box (van Doorne and Westerweel, 2007) made of Plexiglas, filled with glycerol (n=1.47) around the contraction.

The mass flow rate is monitored by a Coriolis mass flowmeter set in different regimes with a variable speed motor-driven that controls the centrifugal pump rotation. Also, the mass flowmeter provides online the temperature and density of the fluid. Seven pressure taps of a 1 mm internal diameter are located along the pipe, four before and three ahead of the contraction plane. The pressure tappings are connected to special chambers and valves, associated with tubbings that are filled with the working fluid and connected to the pressure transducer. Valves are used to set different pressure measurements configurations at each section of the pipe. Gauge pressure at one single point can be obtained using a reference gauge pressure meter. Then, the gauge pressure at the others locations are obtained through the differential measurement related to the pressure reference. All the variables measured by sensors were captured and processed with LabView software ®.

The two dimensional PIV system used to capture the velocity field and some details of the experimental arrangement are showed in the Figure 3a. Figure 3a shows the laser mounted in an optical table and the camera, these positioned forming a 90° angle between their axes. The optical table was mounted in special aluminium structure that

also provides stability and facility to position the camera. The measurements were made approximately 220D far from the inlet.

The PIV acquisition system consisted of a CMOS camera synchronized with the dual cavity Nd:YAG laser. The laser sheet is formed by cylindrical lens allocated into laser head. A 60 mm lens is attached to the camera. In order to improve the particle images quality, a thread camera filter (570 nm) located in the camera lens is used. PMMA-Rhodamin B fluorescence particles with a 10 μm mean diameter are used as a sedding particles in the working fluid. Thus, the light from particles can be easily filtered without reflections because the maximum emission light by particles is in the range of 560 to 590 nm and normal environment reflections has 532 nm.

Even though the use of the visualization box improves the quality of image and the acquisition, some barrel effect causing image distortions still remains. Thus, it was necessary to design an especial calibration grid to "dewarp" the images. With the "dewarping" procedure, explained by many authors (Soloff *et al*, 1997), the perspective and barrel effects can be corrected. The calibration grid shown in Figure 3b was designed considering some advices given in Dynamics Studio (2006). The calibration grid is inserted inside the upstream region of the contraction as shown in Figure 3c.

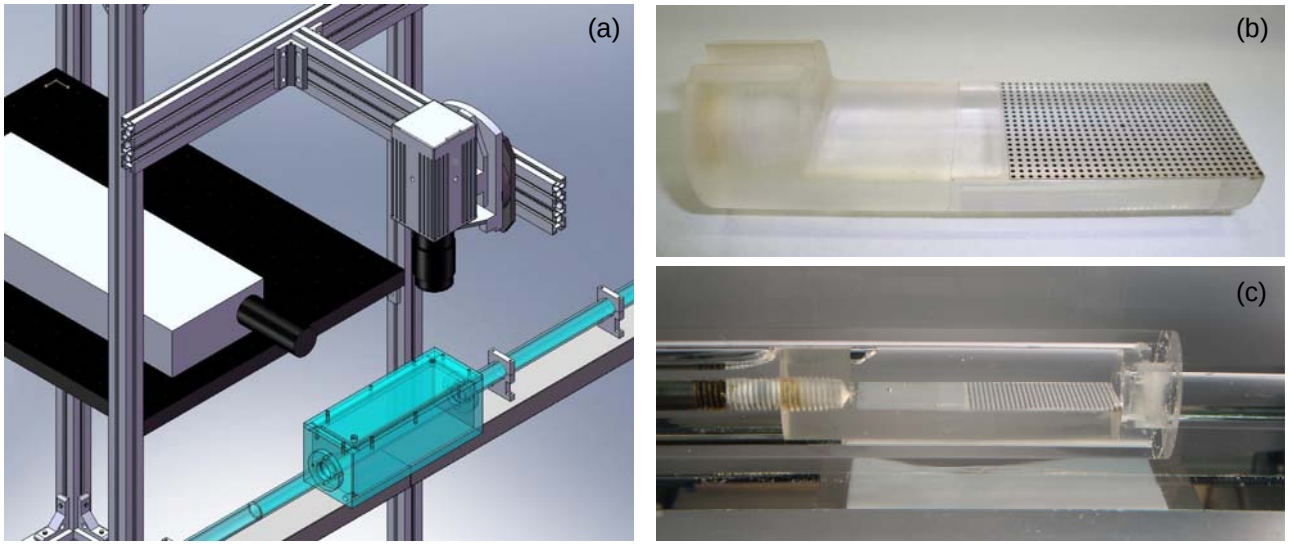

Figure 3. Test Section Details (a) Schematic view of test section. (b) Photo of the calibration grid and its holder. (c) Photo of calibration grid inside test section.

In the image acquisition procedure was used a 60 mJ/pulse energy of the sheet laser light, a 2.8 f-number of the camera, a visual resolution of 2185×1752 px and a 29.8×23.9 mm^2 viewing area. The image pairs captured by the camera are processed by Dynamics Studio 2.3 software. An adaptive correlation with a 32×32 px final interrogation area, 50% window overlap, high accuracy subpixel refinement and central difference interrogation area offset, were used to process the 1047 pair of images of each acquisition. PIV acquisition system was set for different parameter values dependent on the flow conditions. These parameters are chosen considering the limitations of the equipment (maximum repetition rate of the camera and laser), and must be considered which flow scales are necessary to solve (Lumley, 1970). As the flow statistics is solved in the present work, it was chosen a time between frames (camera repetition rate) smaller than the integral time scale of the flow (D/U). In addition, the time-delay between two consecutive passages of the laser beam (image exposure time) was chosen to consider approximately the recommended value of mean in-plane particle displacement by Keane and Adrian (1990) which correspond about 1/4 of interrogation area width (32/4 = 8px). Details of these parameters and the Reynolds value studied are shown in Table 1.

Table 1. Experimental parameters for PIV acquirements.

Upstream Reynolds Number Re_D	Camera repetition rate (Hz)	Image exposure time-delay (μs)
40,000	70	22
24,600	42	37
17,800	30	52

The vector maps obtained were analyzed to detect and replace spurious vectors. In order to efficiently evaluate the total of (105×138×1,047=) 15,171,030 velocity vectors, it was developed a Matlab script according to the methodology proposed by Westerweel and Scarano (2005) and some advices given by Westerweel (2010). Also, the script was used to calculate the average velocity vector, turbulence intensities and others important flow parameters.

4. RESULTS

In this section are presented and discussed the results for pressure loss through the contraction and the velocity field in the upstream contraction section, both calculated numerically and experimentally. For 8 Reynolds numbers, namely, 15,000, 17,800, 20,000, 24,600, 28,000, 32,000, 36,000 and 40,000 were measured experimentally the pressure loss coefficients. Also, 3 Reynolds numbers, namely, 40,000, 24,600 and 17,800, were studied experimentally using the PIV technique and numerically, in order to compare the velocity profiles in different locations along the upstream region and the pressure loss coefficients. In these tests, the recirculation zones close to the contraction plane were investigated.

4.1 Pressure drop and pressure loss coefficient results

The pressure drop is analyzed using the pressure loss coefficient of the contraction, k_c, as a function of the downstream Reynolds number, which is defined as $\mathrm{Re}_d = \rho \bar{V}_2 d / \mu$, where $\bar{V}_2$ is the bulk velocity in the downstream region. In order to calculate experimentally k_c using pressure values measured, it is necessary to calculate P_1 and P_2 pressures values. The convention used by many researchers (Fester *et al*, 2008) is shown in Figure 1b, and it consists in extrapolating the pressure gradients of the fully developed upstream and downstream flow. In the experimental investigation approximately 95 independent pressure samples were measured at each pressure tap point. Several checks were performed to verify the accuracy of results and to ensure that fully developed and redeveloped flow have been reached. Also, it was calculated the friction velocity from pressure measurements according to

$$v^* = \sqrt{\frac{D}{4\rho}\frac{\Delta p}{\Delta z}} \tag{8}$$

where D is the diameter of the pipe, Δp is the measured pressure difference and Δz is the distance over which Δp is measured. The relation between v^* as determined from the pressure differences and the flow rate measurements, always obeyed the Blasius friction law within a 3% error. This is an indication that the flow was indeed fully developed in the upstream and downstream sections. This affirmation was also confirmed by plotting and comparing the readings, as showed in Figure 4a. The results indicate a linear decrease of the mean pressure as function of the axial direction in both sections (den Toonder and Nieuwstadt, 1997). The lines of pressure drop in the upstream and downstream region have been obtained by a linear least square fit method.

The experimental turbulent pressure loss coefficients calculated with pressure data are shown in the Figure 4b as a function of the downstream Reynolds numbers. The coefficients were compared with semi-empirical model developed by McNeil and Morris (1995), the numerical study by IHS ESDU (2005) and the experimental data from Fester *et al.* (2008). Reasonable agreements and coherent tendency were found with McNeil and Morris (1995).

The results show that the loss pressure coefficient is influenced by the downstream Reynolds number, showing a slight decrease with increasing Reynolds number. On the other hand, it was performed a comparison between experimental data and numerical results which are shown in Table 2. It is shown that numerical results obtained with k-ε-LB model are much better than the LVEL ones, specially for higher Reynolds numbers.

Table 2. Comparison of experimental and numerical values of pressure loss coefficients.

Upstream Reynolds Number, Re_D	Pressure loss coefficient value, k_c				
	Experimental	Numerical k-ε-LB	Error %	Numerical LVEL	Error %
40,000	0.4795	0.4715	1.67	0.3382	29.46
24,600	0.5257	0.4916	6.50	0.3367	35.97
17,800	0.5362	0.4488	16.30	0.3299	38.46

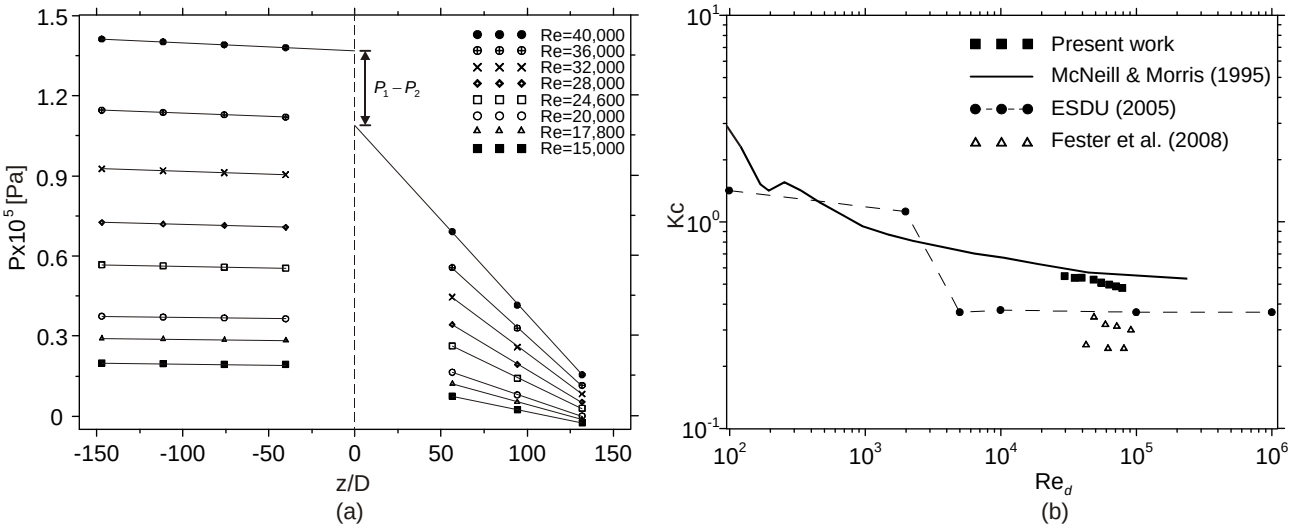

Figure 4. Pressure droop measurements. (a) Pressure measurements along the upstream and downstream sections. (b) Variation and comparison of pressure loss coefficient with upstream Reynolds number.

4.2 Contour maps, streamlines and recirculation zone results

PIV data was used to plot contour maps of the velocity field and some streamlines through the upstream contraction section and the results are depicted in the Figure 5. The velocity magnitude is defined as $V = \sqrt{u^2 + v^2}$, being adimensionalized with the upstream bulk velocity $\overline{V}_1$.

Even though only small differences in the dimensionless velocity vectors can be noticed for the different Reynolds numbers, it can be seen in Figure 5a that dimensionless velocities are dependent of the Reynolds number, presenting the higher values for the highest Reynolds number. From streamlines, it is possible to observe the fluid behavior in the test section. Streamlines show stationary vortexes, which appear in the region near to the sudden contraction for all Reynolds number studied. The region affected by vortex is located immediately before of the contraction plane. From Figure 5b, is observed that the vortex size is a function of the Reynolds number, increasing according to decreasing of Reynolds number. Rama Murthy and Boger (1971) also founded these observations for low Reynolds number.

4.3 Velocity profile results

The average axial and radial velocities profiles of 1,047 instantaneous velocity vectors for 3 Reynolds numbers ($\mathrm{Re}_D = 40{,}000$, 24,600 and 17,800) are presented in this section. The results of velocity vectors for streamwise (axial) and spanwise (radial) directions obtained numerically and experimentally are shown in Figure 6. In the right side are presented axial velocity profiles (u) and in the left are showed radial velocity profiles (v), both adimensionalized by the bulk upstream velocity $\overline{V}_1$, and the z-axis represents the dimensionless positions as a function of upstream diameter D. In order to facilitate the analysis of the results for radial velocities v, their signals have been inverted in the positive r-axis.

Figure 6. presents the good agreement between the experimental and numerical results obtained for all velocity profiles analyzed. It is evident that better results were obtained for k-ε-LB numerical model when compared with experimental data. Also, some differences between numerical and experimental data were found near the contraction plane. Also, it is noted that numerical results are higher than their corresponding experimental values. It can be deduced from axial velocity profiles that measured velocities are symmetrical with respect to centerline and the velocity profiles will be increasingly influenced by the proximity of contraction. On the other hand, the radial velocity increases of points near to the contraction corner and in the centerline, the radial velocities are minimal.

Other observation from the experimental results was referred to maximum velocity value as a function of the Reynolds number. It was observed that dimensionless velocity slightly increases while the Reynolds decreases. Velocity measurements showed that the axial centerline velocity presented the highest value of 3.35 for $\mathrm{Re}_D = 40{,}000$ and this value increases to 3.45 for $\mathrm{Re}_D = 17{,}800$. In the same way, dimensionless radial velocities increases from 2.48 for $\mathrm{Re}_D = 40{,}000$ to 2.55 for $\mathrm{Re}_D = 17{,}800$ for values near to the entry corner of the contraction. Durst and Loy (1985) also verified these outcomes for laminar regimes.

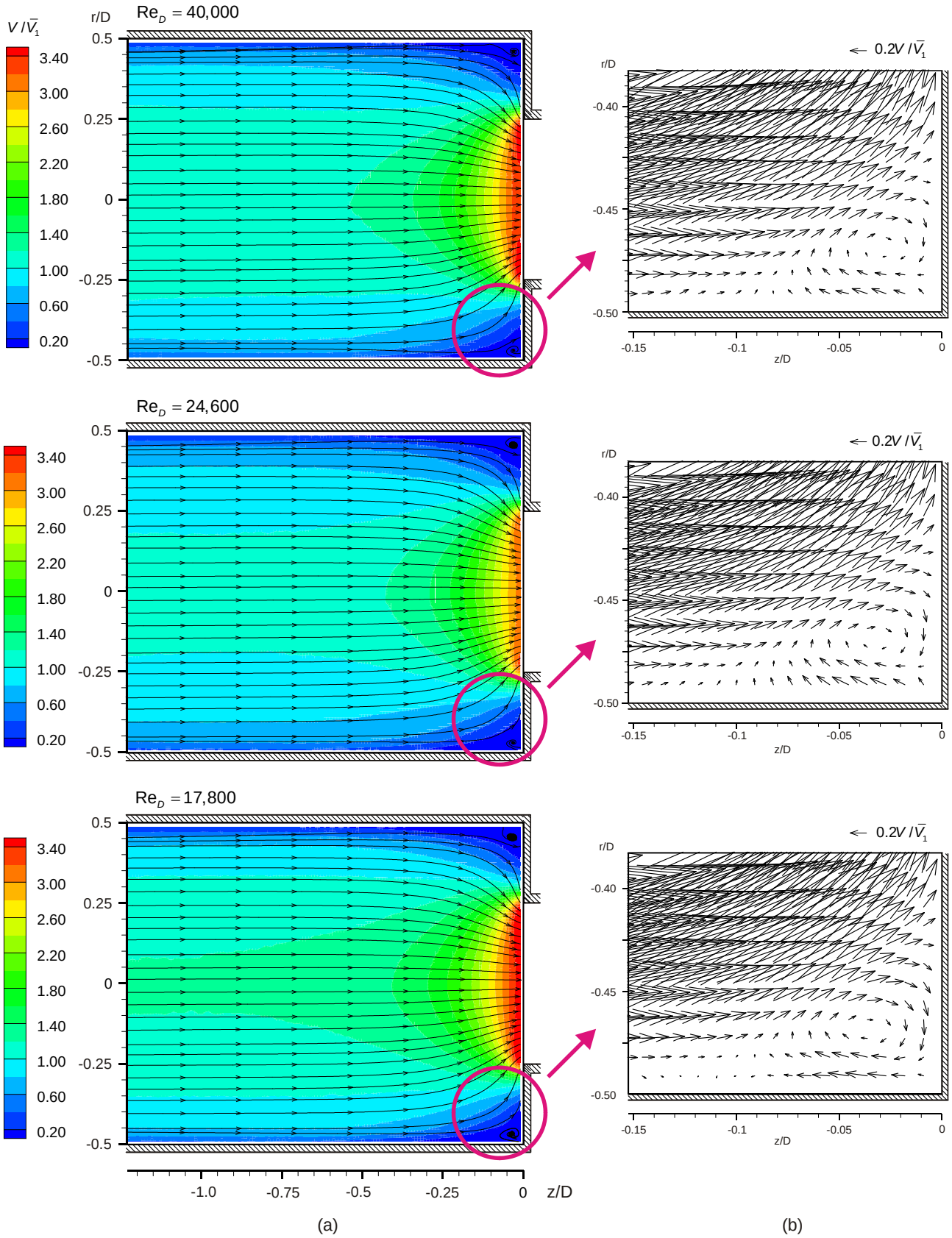

Figure 5. PIV measurements values as function of Re_D for: (a) Contour maps and streamlines. (b) Vortex details.

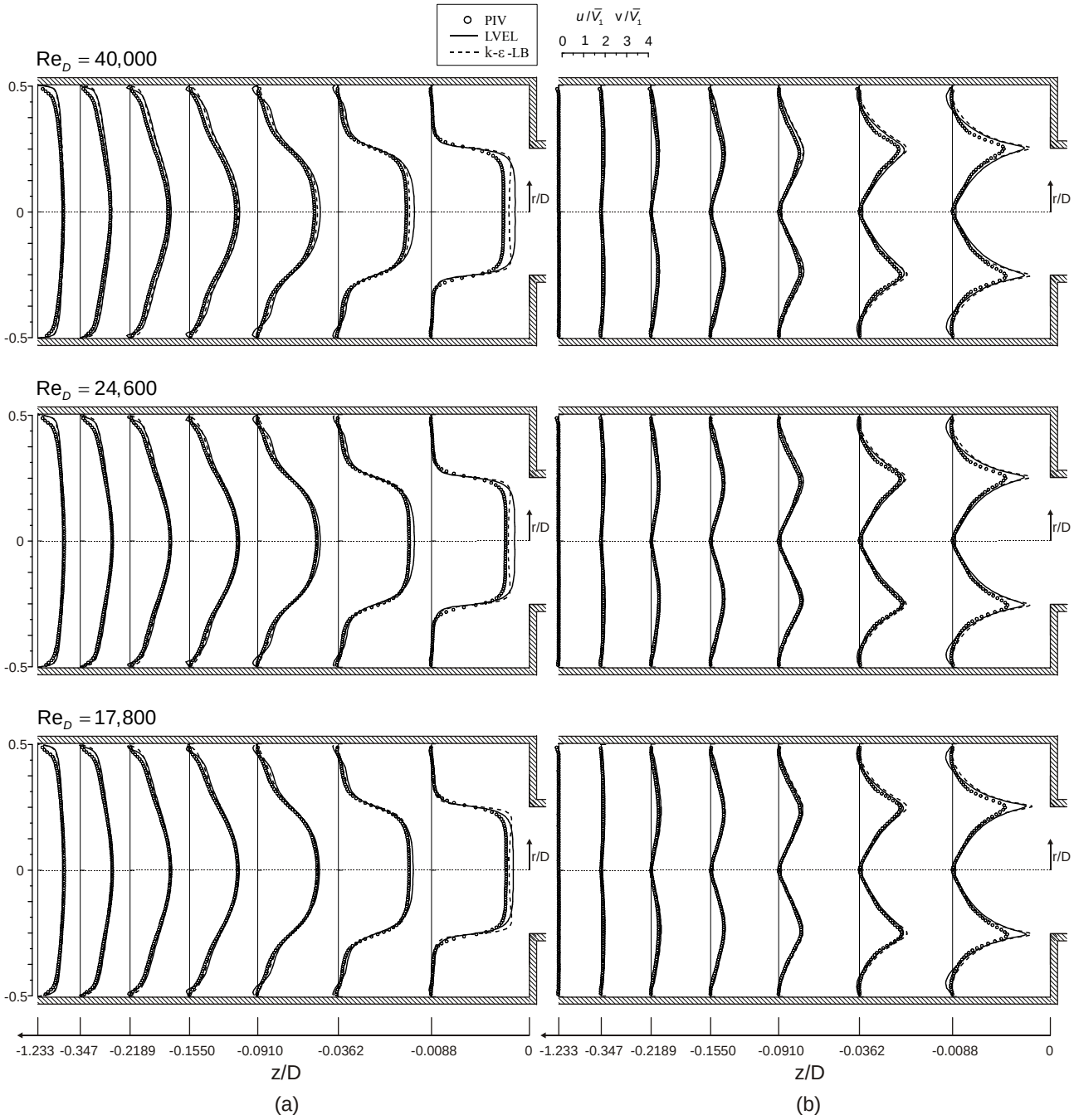

Figure 6. Comparison of numerical and experimental velocity profiles for different Re_D values. (a) Axial velocity profiles. (b) Radial velocity profiles.

5. CONCLUSIONS

In this paper, we investigated numerically and experimentally the Newtonian turbulent flow through a sudden contraction of contraction ratio $\beta = 1.97$. The experimental velocity fields were measured with the PIV technique and for the numerical solution, two turbulence models were used: LVEL and k-ε-LB. Additionally, the pressure loss coefficients were measured and compared with results from literature.

From numerical solution, it was observed an excellent agreement between the axial and radial velocity profiles obtained with the two turbulence models: L-VEL and k-ε-LB. The comparison between numerical and experimental results using PIV technique was very satisfactory. The discrepancies between the maximum velocities obtained numerically and experimentally increase as the flow approaches the contraction plane. In general, the best numerical results when compared with the experimental ones were obtained with k-ε-LB turbulence model.

Compared with the literature, the experimental pressure loss coefficient presented consistent values. From comparison between experimental and numerical results it was observed that the smallest deviations are found with k-ε-LB turbulence model.

Regarding the vortex located just before the plane of contraction, one observed experimentally that its size or area of influence increases with decreasing Reynolds number in the range studied.

Finally, the results provide reliable experimental values and physically consistent, velocity profiles and pressure loss coefficients. These data extends the results available in literature and it can be used to validate numerical models and experimental studies, on a range of Reynolds poorly investigated.

6. ACKNOWLEDGEMENTS

The authors acknowledge the financial support of FINEP/CTPetro, National Agency for Petroleum, Natural Gas and Biofuels (ANP) through its Human Resources Program (UTFPR/PRH-10) and CENPES/PETROBRAS.

7. REFERENCES

Astarita, G. and Greco, G., 1968, "Excess Pressure Drop in Laminar Flow through Sudden Contraction", Industrial & Engineering Chemistry Fundamentals, 7: 595-598.

Bullen, P.R., Cheeseman, D.J., Hussain, L.A. and Ruffellt A.E., 1987, "The Determination of Pipe Contraction Pressure Loss Coefficients for Incompressible Turbulent Flow", International Journal of Heat and Fluid Flow, 8: 111-118.

Bullen, P.R., Cheeseman, D.J., Hussain, L.A. and Ruffellt A.E., 1996, "A Study of Turbulent Pipe in Pipe Contractions", Journal of Process Mechanical Engineering, 210: 171-180.

Dantec Dynamics, 2006. "3D Stereoscopic PIV Reference Manual", 8th Ed, Skovlunde, Denmark.

Den Toonder, J.M.J. and Nieuwstadt F.T.M., 1997, "Reynolds Number Effects in a Turbulent Pipe Flow for Low to Moderate Re", Physic of Fluids, Vol. 9, 11: 3398-3409.

Durst, F. and Loy, T., 1985, "Investigation of Laminar Flow in Pipes with a Sudden Contraction of Cross Sectional Area", Computers & Fluids, 13: 15-36.

Fester, V. Mbiya B and Slatter P., 2008, "Energy Losses of non-Newtonian Fluids in Sudden Pipe Contractions", Chemical Engineering Journal, 145: 57-63.

IHS ESDU, 2005, "Flow through Sudden Contractions of Duct Area: Pressure Loss and Flow Characteristics", ESDU 05024.

Keane, R.D. and Adrian, R.J., 1990, "Optimization of Particle Image Velocimetry. Part I: Double Pulsed Systems", Meas. Sci. Technol., 2: 1202-1215.

Lam, C.K.G. and Bremhorst, K.A., 1981, "A Modified Form of the k-ε Model for Predicting Wall Turbulence", Journal of Fluids Engineering, 103: 456-460.

Launder B.E. and Spalding D.B., 1974, "The Numerical Computation of Turbulent Flows", Computer Methods in Applied Mechanics and Engineering, 3: 269-289.

Lumley, J.L., 1970, "Stochastic Tools in Turbulence", Academic Press, 1970 edition, New York, USA.

McNeill, D.A. and Morris S.D., 1995, "A Mechanistic Investigation of Laminar through an Abrupt Enlargement and Nozzle and its Applications to Other Pipe Fittings", Report EUR 16348 EN, 13: 15-36.

Patankar, S.V. and Spalding, D.B., 1972, "A Calculation Procedure for Heat, Mass and Momentum Transfer in Three-Dimensional Parabolic Flows", International Journal of Heat and Mass Transfer, 15: 1787-1806.

Rama Murthy A.V. and Boger D.V., 1971, "Developing Velocity Profiles on the Downstream Side of a Contraction for Inelastic Polymer Solutions", Transactions of the Society of Rheology, 15:4, 709-730.

Soloff, S.M., Adrian, R.J. and Liu, Z.C., 1997, "Distortion Compensation for Generalized Stereoscopic Particle Image Velocimetry", Meas. Sci. Technol., 8: 1441-1454.

Van Doorne C.W.H. and Westerweel J., 2007, "Measurements of Laminar, Transitional and Turbulent Pipe Flow Using Stereoscopic-PIV", Experiments in Fluids, 42: 259-279.

Vrentas, J.S. and Duda, J. L., 1973, "Flow of a Newtonian Fluid through a Sudden Contraction", Appl. Sci., 28: 241-260.

Westerweel J. and Scarano F., 2005, "Universal Outlier Detection for PIV Data", Experiments in Fluids, 39: 1096-1100

Westerweel J., 2010, Private Communication.

White, F.M., 2002, "Mecânica dos Fluidos", Editora McGraw-Hill, 4ª Ed, Rio de Janeiro, Brazil.

Wilcox, D.C., 1998, "Turbulence Modeling for CFD", DCW Industries, 2ª Ed, California, USA.

8. RESPONSIBILITY NOTICE

The authors are the only responsible for the printed material included in this paper.